Cell Calcium 80 (2019) 152–159

Contents lists available at ScienceDirect

Cell Calcium

journal homepage: www.elsevier.com/locate/ceca

Monomeric state of S100P protein: Experimental and molecular dynamics study

Sergei E. Permyakov[a,*], Alexander I. Denesyuk[a,b], Konstantin A. Denessiouk[b,c], Maria E. Permyakova[a], Alixey S. Kazakov[a], Ramis G. Ismailov[a], Victoria A. Rastrygina[a], Andrei S. Sokolov[a], Eugene A. Permyakov[a,*]

[a] Institute for Biological Instrumentation of the Russian Academy of Sciences, Federal Research Center 'Pushchino Scientific Center for Biological Research of the Russian Academy of Sciences', Pushchino, Moscow region 142290, Russia
[b] Structural Bioinformatics Laboratory, Faculty of Science and Engineering, Åbo Akademi University, Turku 20520, Finland
[c] Pharmaceutical Sciences Laboratory, Faculty of Science and Engineering, Pharmacy, Åbo Akademi University, Turku 20520, Finland

ARTICLE INFO

Keywords:
S100P protein
Monomeric S100P
Interleukin
Molecular dynamics
EF-hand

ABSTRACT

S100 proteins constitute a large subfamily of the EF-hand superfamily of calcium binding proteins. They possess one classical EF-hand Ca^{2+}-binding domain and an atypical EF-hand domain. Most of the S100 proteins form stable symmetric homodimers. An analysis of literature data on S100 proteins showed that their physiological concentrations could be much lower than dissociation constants of their dimeric forms. It means that just monomeric forms of these proteins are important for their functioning. In the present work, thermal denaturation of apo-S100P protein monitored by intrinsic tyrosine fluorescence has been studied at various protein concentrations within the region from 0.04–10 μM. A transition from the dimeric to monomeric form results in a decrease in protein thermal stability shifting the mid-transition temperature from 85 to 75 °C. Monomeric S100P immobilized on the surface of a sensor chip of a surface plasmon resonance instrument forms calcium dependent 1 to 1 complexes with human interleukin-11 (equilibrium dissociation constant 1.2 nM). In contrast, immobilized interleukin-11 binds two molecules of dimeric S100P with dissociation constants of 32 nM and 288 nM. Since effective dissociation constant of dimeric S100P protein is very low (0.5 μM as evaluated from our data) the sensitivity of the existing physical methods does not allow carrying out a detailed study of S100P monomer properties. For this reason, we have used molecular dynamics methods to evaluate structural changes in S100P upon its transition from the dimeric to monomeric state. 80-ns molecular dynamics simulations of kinetics of formation of S100P, S100B and S100A11 monomers from the corresponding dimers have been carried out. It was found that during the transition from the homo-dimer to monomer form, the three S100 monomer structures undergo the following changes: (1) the helices in the four-helix bundles within each monomer rotate in order to shield the exposed non-polar residues; (2) almost all lost contacts at the dimer interface are substituted with equivalent and newly formed interactions inside each monomer, and new stabilizing interactions are formed; and (3) all monomers recreate functional hydrophobic cores. The results of the present study show that both dimeric and monomeric forms of S100 proteins can be functional.

1. Introduction

S100 proteins constitute a large subfamily of the superfamily of EF-hand calcium binding proteins [1,2]. All the proteins within this superfamily have a common structural domain (EF-hand) consisting of a Ca^{2+}-binding loop flanked by two α-helices [1–3]. S100 proteins are the smallest members of the EF-hand superfamily and their molecules consist of only two EF-hand domains. Acidic amino acid residues within the Ca^{2+}-binding loop provide ligands for Ca^{2+} binding in a pentagonal, bipyramidal fashion. The C-terminal EF-hand of S100 s is canonical and binds calcium with dissociation constant, $K_d \approx 10$ to 50 μM [1]. The N-terminal EF-loop has two more residues (14 instead of 12) in

Abbreviations: IL-11, interleukin-11; rWT IL-11, recombinant human interleukin-11omitting the N-terminal Pro residue of the mature protein (residues 23–199 of Swiss-Prot entry P20809); S100P, recombinant human S100P; SPR, surface plasmon resonance; RU, resonance unit

* Corresponding authors at: Protein research group, Institute for Biological Instrumentation of the Russian Academy of Sciences Federal Research Center "Pushchino Scientific Center for Biological Research of the Russian Academy of Sciences", Institutskaya str., 7, Pushchino, Moscow region, 142290, Russia.
E-mail addresses: permyakov.s@gmail.com (S.E. Permyakov), epermyak@yandex.ru (E.A. Permyakov).

https://doi.org/10.1016/j.ceca.2019.04.008
Received 11 March 2019; Received in revised form 13 April 2019; Accepted 27 April 2019
Available online 29 April 2019
0143-4160/

comparison with the canonical EF-hand and many of its ligands for calcium are backbone carbonyl oxygen atoms rather than oxygens of side chain Asp or Glu residues as is typically found in the canonical EF-hand [4]. Most of the S100 proteins form stable symmetric homodimers.

S100 proteins regulate many intracellular and extracellular activities including protein phosphorylation and enzyme activity, gene transcription, dynamics of cytoskeleton components, and cell proliferation and differentiation [1,2].

An analysis of literature data on S100 proteins showed that their physiological concentrations in serum could be much lower than dissociation constants of their dimeric forms (see Table 1S) [40–46]. One can assume that in some cases, when S100 proteins perform some functions in extracellular medium, monomeric forms of these proteins can to be important for their functioning. For this reason, in order to reveal functional properties of these proteins one should study the structure and properties of their monomeric states, which is hard to do because of very low values (sometimes in nanomolar range) of dissociation constants of S100 dimers. Monomeric S100 proteins are formed at very low protein concentrations (less than 10^{-8} M) and it does not allow studying them by most physical and chemical methods. For this reason in order to study character of conformation changes induced by dissociation of S100 dimers into monomers one can use molecular dynamics methods.

For our studies we have chosen one of the members of the S100 family S100P, a 95-amino-acid protein first extracted from placenta [5,6]. Expression of S100P was found in various cancer cell lines and there is accumulating evidence that it is overexpressed in a number of solid tumors. S100P protein seems to play a significant role in the development and progression of various cancers [1], [2]. Increased levels of S100P have been observed in multiple tumor cell lines and breast, pancreas, lung and ovary carcinomas [7]. A number of microarray and immunohistochemical studies have shown that S100P transcription and protein expression correlate with characteristic features of malignant phenotype in various types of tissues [8].

S100P protein has two Ca^{2+}-binding sites; one with high affinity (canonical) (K_d 1.6 μM) and the other one with lower affinity (non-canonical) (K_d 800 μM) [5]. The secondary structure of the S100P protein is insignificantly affected by the binding of calcium but its tertiary structure is altered considerably resulting in an exposure of hydrophobic surfaces [9,10] and this is related to dimer formation [11]. These conformational changes activate the protein and render a conformation that is capable of binding other proteins.

S100P exists as a homodimer formed by non-covalent interactions between large hydrophobic areas of monomers [12]. Koltzscher and Gerke [13] identified conserved hydrophobic amino acid residues involved in dimerization of S100 P. Using an indirect method, they found that F15 is crucially important for dimerization since its substitution by alanine abolishes the dimerization. Our results obtained by a direct point mutation method showed that this is not true [14]. According to the data of Koltzscher and Gerke [13], I11, I12, or F89 need to be replaced by a less hydrophopic residue in both subunits of S100P for serious disturbance of the dimerization. Zhang et al. [12] showed that the association kinetics of S100P dimer is faster in the presence of calcium than in their absence, whereas its dissociation rate constant is independent of calcium. Equilibrium dissociation constant values for S100P dimers are 64 nM and 2.5 μM in the presence and in the absence of calcium ions, respectively.

In the present work, we studied dissociation of the S100P dimers into monomers by experimental and molecular dynamics methods and found that the structure and physical properties of S100P protein in monomeric and dimeric form are essentially different.

2. Materials and methods

2.1. Materials

ProteOnTM GLH Sensor Chip and Amine Coupling Kit were from Bio-Rad Laboratories. Biology grade HEPES, ultra-grade H_3BO_3 and BioUltra-grade glycine were from Calbiochem, Fluka, and Sigma-Aldrich Co, respectively. Ultra-pure grade Tris, high pure-grade PMSF and ultra-pure grade Tricine were purchased from Amresco. Biotechnology grade DTT was bought from DiaM (Moscow, Russia). USP grade sodium chloride, molecular mass markers for SDS-PAGE, were from Helicon (Moscow, Russia). Sephadex G-25 was product of Pharmacia LKB. Ultra-grade EDTA and EGTA were from Sigma-Aldrich Co. Other chemicals were reagent grade or higher.

All buffers and other solutions were prepared using ultrapure water (Millipore Simplicity 185 system). Plastic or quartz ware was used instead of glassware, to avoid contamination of protein samples with Ca^{2+}. Thermo SnakeSkin dialysis tubing (3.5 kDa MWCO) was used for dialysis of protein solutions.

2.2. Methods

2.2.1. Expression and purification of recombinant IL-11 and S100P

Recombinant human IL-11 (rWT IL-11) and human S100P were prepared as previously described [15]. Protein concentrations were measured spectrophotometrically using molar extinction coefficients at 280 nm calculated according to [16]: 17,990 $M^{-1}\,cm^{-1}$ and 2980 $M^{-1}\,cm^{-1}$, for rWT IL-11 and S100P, respectively.

2.2.2. Preparation of apo-protein

The purification of human S100P samples from calcium ions was performed using the Sephadex G-25 gel filtration method [17]. A sample of 4–5 mg of lyophilized human S100P was dissolved in 10 mM HEPES-KOH, 20 mM EDTA, pH 8.0 and loaded onto 1.0 × 20 cm Sephadex G-25 column equilibrated with 10 mM HEPES-KOH, 20 mM EDTA, pH 8.0. Elution rate was 0.2 ml/min.

2.2.3. Fluorescence measurements

Fluorescence studies were carried out on a Cary Eclipse spectrofluorimeter (Varian, Inc.) equipped with a Peltier controlled cell holder. Quartz cells with pathlength of 10 mm were used. All spectra were corrected for spectral sensitivity of the instrument. Spectrofluorimetric temperature scans were performed stepwise allowing the sample to equilibrate at each temperature. The average heating rate was 1 °C/min. Temperature was monitored inside the cell. Excitation wavelength was 270 nm. Spectra were recorded from 290 nm to 370 nm. Protein concentration in fluorescent measurements was from 10 μM to 20 nM. All manipulations with the protein were carried out only in quartz and plastic tubes. The prepared protein solutions were kept over 10 h at + 4 °C. Before measurements, the protein solution was transferred into a fluorescent cell and degassed using degassing station (TA Instruments) for 10 min with constant stirring. Mid-temperature of thermally induced transitions for each protein concentration was determined as the average of the mid-temperature thermal transitions monitored by fluorescence intensities at 300, 306 and 330 nm. Mid-temperatures of the thermal transitions for various protein concentrations in the region from 0.04–10 μM were obtained by the method described by Permyakov, [18,19].

2.2.4. Evaluation of dissociation constant of S100P dimers

The scheme of protein dimerization is:

$$P \leftrightarrow D \qquad (I)$$

where P is monomer and D is dimer. Let S is an experimentally determined parameter proportional to the population of P

$$S = \alpha_p \times S_p + (1 - \alpha_p) \times S_D;\ \alpha_p = [P]/P_0 \quad (1)$$

where α_p is a portion of the protein in the monomeric state, S_P and S_D are values of S corresponding to the pure P and D forms, respectively, P_0 is a total monomer concentration.

Equilibrium dimerization constant:

$$K = [D]/[P]^2 \quad (2)$$

Then,

$$[D] = K \times [P]^2 \quad (3)$$

Let's put [D] to the material balance equation:

$$P_0 = [P] + 2[D] \quad (4)$$

$$P_0 = [P] + 2K \times [P]^2 \quad (5)$$

$$2K \times [P]^2 + [P] - P_0 = 0 \quad (6)$$

$$[P] = [(1 + 8\,K \times P_0)^{1/2} - 1]/4\,K \quad (7)$$

If we have an experimental dependence of S on P_0 we can evaluate dissociation constant K fitting the theoretical Eq. (1) to the experimental data by means of variation of the fitting parameters K, S_P and S_D.

2.2.5. Scanning calorimetry measurements

The scanning calorimetry studies were carried out on a Nano DSC microcalorimeter (TA Instruments) at a 1 K/min heating rate and excess pressure of 4 bar (20 mM Glycin-KOH, pH 9.2, 1 mM EGTA buffer for apo-state of rWT human S100P; 20 mM H_3BO_3-KOH, pH 8.3, 1 mM $CaCl_2$ buffer for Ca^{2+}-loaded state of rWT human S100P). S100P concentrations were 1.5–2 mg/ml. The protein specific heat capacity (C_p) was calculated as described by Privalov and Potekhin [20]. The partial molar volume of S100P and specific heat capacity of the fully unfolded protein were estimated according to Hackel et al. [21] and Makhatadze et al. [22], respectively. The temperature dependence of C_p was analyzed according to either the cooperative two-state model:

$$n{\cdot}N \leftrightarrow n{\cdot}D \quad (II)$$

where N and D denote native and denatured protein states, respectively; n is a number of molecules involved in the transition (cooperativity of thermal transition). The experimental data were fitted by theoretical curves using Microcal OriginPro 8.0 (OriginLab Corporation, Northampton, MA, USA) software [23]. The heat capacity change accompanying transition (ΔC_p) was supposed to be independent of temperature. ΔC_p, mid-transition temperature (T_0), enthalpy of protein denaturation at temperature T_0 (ΔH_0), and n for the model [II] were used as fitting parameters (in some cases n was set to 1).

2.2.6. Surface plasmon resonance studies

Surface plasmon resonance (SPR) measurements were performed at 25 °C using ProteOn™ XPR36 protein interaction array system and ProteOn GLH sensor chip (Bio-Rad Laboratories, Inc.). Ligand (40 μg/ml human rWT S100P in 10 mM sodium acetate, pH 4.5 buffer) was immobilized on the chip surface (up to 10,000 resonance units, RUs) by amine coupling, according to the manufacturer's instructions. The remaining activated amine groups on the chip surface were blocked by 1 M ethanolamine solution. In order to obtain immobilized S100P monomer the sensor chip with the immobilized S100P dimer was treated by passage of 0.5% SDS water solution for 50 s and then by 10 mM sodium acetate, pH 4.5 buffer. Analyte (human rWT IL-11, 69 nM to 553 nM) in running buffer (10 mM HEPES, 150 mM NaCl, 0.01% TWEEN 20, pH 7,4 buffer with 1 mM $CaCl_2$) was flowed over the chip at 30 μl/min for 350 s, followed by flushing the chip with the running buffer for 2400 s. The double-referenced SPR sensograms were globally fitted according to the single site binding scheme (Langmuir):

$$L + A \underset{k_d}{\overset{k_a}{\leftrightarrow}} LA; \quad (III)$$

where k_a and k_d refer to kinetic association and dissociation constants, respectively. Constants were evaluated using ProteOn Manager™ v.3.1 software (Bio-Rad Laboratories, Inc.). The sensor chip surface was regenerated by passage of 0.5% SDS water solution for 50 s.

2.2.7. Molecular dynamics simulations

The A and B chains of the best representative conformer 15 of apo-S100P from PDB entry 1OZO [24] were taken for the molecular dynamics simulations using GROMACS software package, version 4.5.4 [25]. These chains were placed in a cubic box of 5.5 nm length using the 'editconf' tool, and solvated with the "SPC" (Simple Point Charge) [26] water model, using the 'genbox' tool. We made all our simulations in the presence of 0.2 M NaCl. Seventeen Na^+ ions and 12 Cl^- ions were added to replace initial SPC waters in all directions, using the 'genion' tool. The final system was initially minimized with 500 steps (1 ps) using the steepest descent algorithm followed by 25,000 steps (50 ps) of the solvent relaxation at 300 K. Temperature (300 K) and pressure (1 atm) were controlled with the Berendsen weak coupling algorithm [27]. Simulation time was 80 ns. Electrostatic interactions were calculated using the Particle-Mesh-Ewald (PME) algorithm [28], a Fourier grid spacing of 0.12 nm and fourth order spline interpolation. Coordinates were recorded every picosecond. The final coordinates of the simulation of monomers and root mean square fluctuations (RMSF) were analyzed using tools available within the GROMACS package. Molecular simulations of structural rearrangements in the A and B chains of the apo-S100B and apo-S100A11 (PDB entries 1CFP (model 1) [29] and 1NSH (model 1) [30], respectively, have been also carried out. The cubic box was generated with volume 6.5 × 6.5 × 6.5 nm^3 in both cases. Randomly chosen water molecules were then replaced by the neutralizing 30 ions of Na^+ and 16 ions of Cl^- in S100B, and 30 ions of Na^+ and 30 ions of Cl^- in S100A11. All other parameters of the simulation protocol were similar to those of S100 P. Interacting surfaces and atomic contacts were calculated using the Contacts of Structural Units (CSU) software [31].

3. Results and discussion

Fig. 1 shows temperature dependencies of specific heat capacities of apo- and Ca^{2+}-bound states for rWT S100P calculated from differential scanning calorimetry data. The heat sorption peaks correspond to the

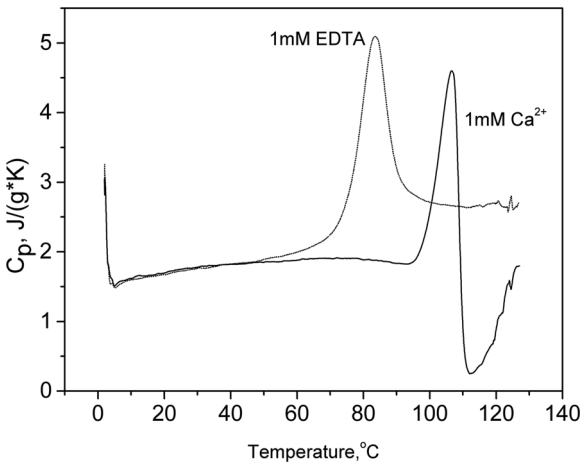

Fig. 1. Temperature dependencies of specific heat capacities of apo- and Ca^{2+}-bound states of rWT S100P calculated from DSC data. Dashed line: apo-rWT S100P, 20 mM Glycin-KOH, 1 mM EGTA pH 9.2; 1.98 mg/ml. Solid line: Ca^{2+}-loaded rWT S100P, 20 mM H_3BO_3-KOH, 1 mM $CaCl_2$, pH 8.3; 1.54 mg/ml.

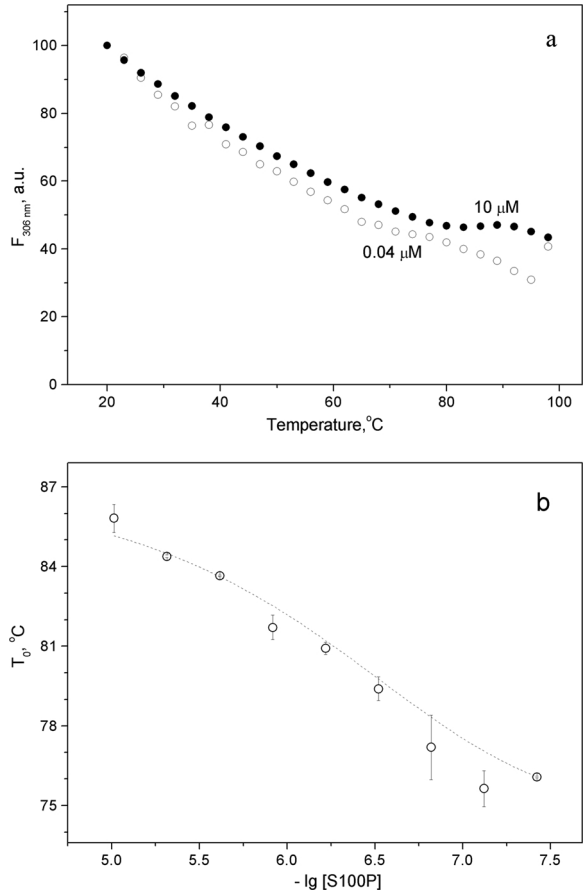

Fig. 2. a – Temperature dependencies of normalized intrinsic tyrosine fluorescence at 306 nm for two different concentrations of apo-S100P protein. b – The dependence of mid-temperature of thermal transition in S100P protein upon logarithm of protein concentration. 10 mM HEPES-KOH, 1 mM EDTA, pH 7.3. Excitation wavelength was 270 nm.

thermally induced unfolding transitions in the protein. In the absence of calcium ions, the peak is located at about 84 °C. The negative peak at higher temperatures corresponds to strong aggregation processes, which distort the heat sorption curve. The binding of calcium shifts the heat sorption peak toward higher temperatures up to 105 °C. The scanning microcalorimetry method requires the use of rather high protein concentration: 1.5–2 mg/ml in our measurements (72–96 μM). Taking into consideration very low dissociation constant of S100P dimers (nanomolar range) both in apo- and Ca^{2+}-loaded states one can conclude that in our measurements the protein was in the dimeric state. At the same time, we would like to study a monomeric state of S100P protein. For this purpose, we should use more sensitive physical method, for example, intrinsic fluorescence method. Unfortunately, S100P protein does not contain tryptophan residues, but contains two tyrosine residues, fluorescence of which can be used for temperature unfolding measurements [19].

Fig. 2A shows normalized temperature dependencies of intrinsic tyrosine fluorescence at 306 nm for two different concentrations of apo-S100P protein (0.04 and 10 μM). The increase in temperature results in common smooth thermal quenching of tyrosine fluorescence but a deflection from it at elevated temperatures reflects a thermal unfolding transition in the protein [19]. The decrease in protein concentration shifts the thermal transition toward lower temperatures. This shift seems to reflect a dissociation of S100P dimers into monomers. Mid-temperatures of the thermal transitions for various protein concentrations in the region from 0.04–10 μM were obtained by the method described in [19,18]. The dependence of mid-temperature of the thermal transition on logarithm of protein concentration is shown in Fig. 2B. The figure shows that the transition from the dimeric to monomeric form of S100P results in a decrease in protein thermal stability shifting the mid-transition temperature from 85 to 75 °C. An effective dissociation constant of S100P dimers evaluated from these data is about 0.5 μM.

We have studied interactions of monomeric form of S100P protein with recombinant interleukin-11 (IL-11) by surface plasmon resonance spectroscopy. Interleukin-11 (IL-11) is a multifunctional hematopoietic cytokine expressed by epithelial cells, fibroblasts and leukocytes [32–34]. IL-11 and S100P are oncoproteins co-expressed in many types of cancers [35,8]. Recently we found that interleukin-11 interacts with S100P in a calcium dependent manner [15]. We revealed that IL-11 and S100P can form both 1:1 and higher order complexes with two dissociation constants of 32 nM and 288 nM, which were assigned to monomeric and oligomeric forms of S100P, respectively [15]. In the present work, S100P protein was immobilized on the surface of a sensor chip by amine coupling and treated by 0.5% SDS to break dimers. As an analyte (running in a liquid phase) we used IL-11. It was found that in the presence of calcium, equilibrium dissociation constant of the complex S100P - IL-11 is about 1.2 nM (Fig. 3, Table 1), which is 30–280 times lower than the constant we measured earlier for dimeric S100P (32 and 288 nM). Moreover, in contrast to the bimodal interaction observed when S100P was an analyte, the interaction of IL-11 with the monomeric S100P can be described by the 1:1 binding scheme, which shows homogenity of the immobilized sample. These results clearly show that IL-11 has only one S100P-binding site and the interaction of monomeric S100P with IL-11 differs from that for oligomeric form. This result is in a good agreement with our recent study of the interaction of S100P with human serum albumin. We showed that this interaction is also calcium-dependent and occurs only with monomeric S100P [36].

Unfortunately, the sensitivity of the existing physical and chemical methods does not allow a detailed study of S100P monomer properties at concentrations less than 10^{-7} M. For this reason, we have used molecular dynamics methods to evaluate structural changes in S100P upon its transition from dimeric to monomeric state.

Currently, Protein Data Bank (PDB; www.rcsb.org, [37] contains two structures of the S100P protein: the NMR structure of the ligand-free S100P homodimer (PDB code 1OZO [24],) and the crystal structure of the calcium-bound S100P monomer (PDB code 1J55 [12];). The homodimer structure of S100P was chosen for the molecular dynamics analysis. Fig. 4 shows ribbon representation of the S100P homodimer in solution, containing two symmetric apo-S100P subunits with four-helix bundles in each of them (conformer 15 in ensemble 1OZO). The two

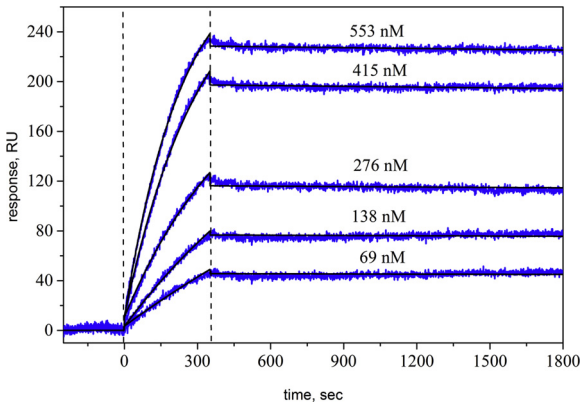

Fig. 3. Kinetics of the interaction of rWT S100P with IL-11 at 25 °C, monitored by SPR spectroscopy (immobilization of S100P on the sensor chip surface by amine coupling). 10 mM HEPES, 150 mM NaCl, 0.05% TWEEN 20, pH 7.4 buffer with 1 mM $CaCl_2$. Blue curves are experimental, while black curves are theoretical, calculated according to the single site binding scheme (1) (see Table 1 for the fitting parameters).

Table 1
Parameters of the interaction between rWT S100P and IL-11 computed according to the single site binding scheme (1) on the base of SPR data (see Fig. 3).

Analyte \Parameter	k_a, M^{-1} s^{-1}	k_d, s^{-1}	K_d, nM	R_{max}, RU	χ^2
Human rWT IL11	(7.71 ± 0.06) × 10^3	(9.79 ± 0.33) × 10^{-6}	1.27 ± 0.03	264	4.33

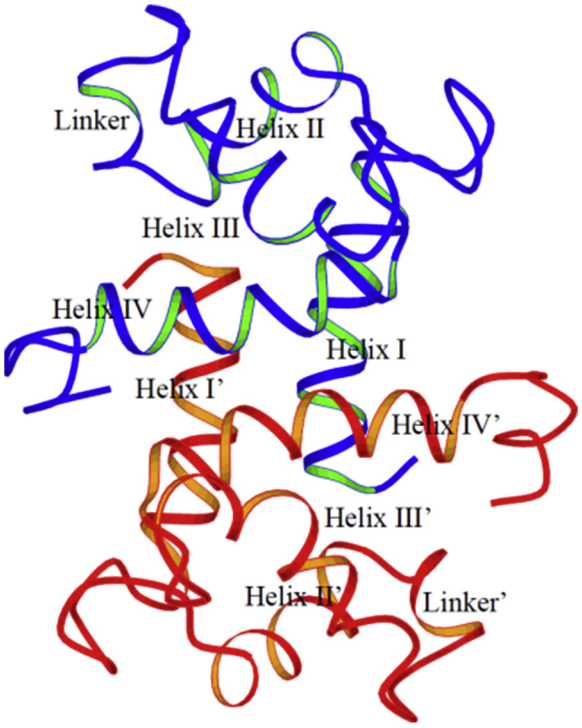

Fig. 4. Ribbon representation of the original NMR structure of the ligand-free S100P homodimer (PDB code 1OZO; [27]) in solution prior to molecular dynamics simulation procedures. The two monomers are shown in red and blue. Helices are numbered according to the 1OZO file. The "Linker" and "Linker'" designations show the loops, which join two EF-hand motifs in each of the two monomers, respectively.

monomers interact with each other in an antiparallel manner with the creation of a "mixed" four helices bundle, constructed from helices I and IV from chain A, and helices I' and IV' from chain B at the interface. The four helices bundle at the homodimer interface is stabilized by three main inter-domain clusters consisting of mostly non-polar residues: a cluster between antiparallel helices I and I'; a cluster between antiparallel helices IV and IV'; and a large cluster between the I/I' helix pair positioned across the IV/IV' helix pair, where helix I interacts with helix IV' and, at the same time, helix I' interacts with helix IV. Other additional inter-domain contacts within the homo-dimer include interactions between the positively charged amino terminus of helix I and the negatively-charged carboxylic terminus of helix II', and symmetrically, between the positively charged amino terminus of helix I' and the negatively charged carboxylic terminus of helix II. Separation of the homodimer into two monomers removes all inter-domain interactions between helices at the dimer interface and leaves all non-polar surfaces of separated helices exposed to the solvent.

The separated S100 monomers are able to exist as globular proteins, if they readjust their conformation to shield hydrophobic surfaces from the solvent and to substitute the lost contacts by new ones. In order to study changes in the conformation of monomers after the separation,

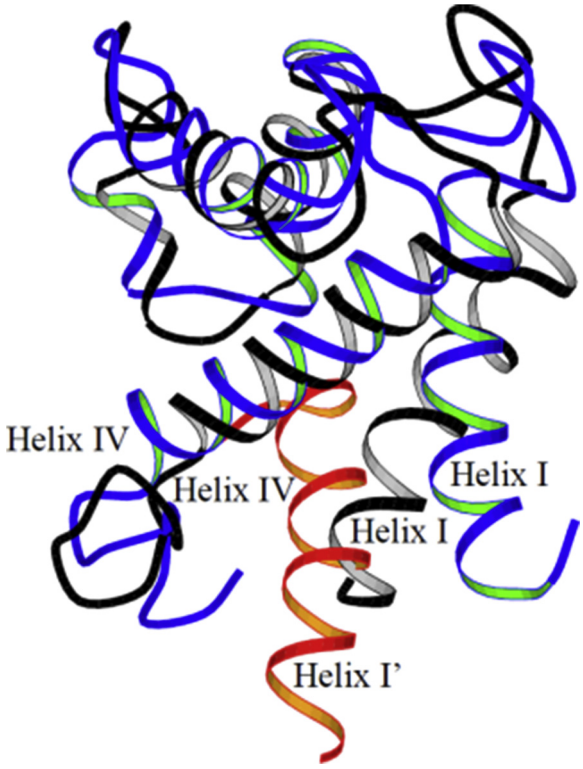

Fig. 5. Structural alignment of the S100P monomers before (blue) and after (black) the 80 ns molecular dynamics simulation. In order to compare positions of the helices I and I' before and after the simulation, position of the helix I' from the second S100P monomer before the simulation (red) is also shown.

we carried out 80-ns kinetic simulations of structural changes for the two apo-S100P monomers in solution. All molecular dynamics simulations were carried out using GROMACS software package [25]. Fig. 5 shows a superposition of the coordinates of the apo-S100P monomer (A chain) before and after the 80-ns simulation. The simulation shows that, indeed, the four helices bundles within each monomer do change their conformations in order to shield the exposed non-polar residues from the solvent. The most noticeable change in the monomer structure is the change in the orientation of helix I/I' with respect to the rest of the bundle. In the separated monomer, the position of the helix I is close to the position of the helix I' in the dimer structure, thus mimicking interactions between helices I' and IV at the dimer interface (shown in red on Fig. 5). In the apo-S100P monomer before simulation, the hydrophobic amino acids of the N-terminal portion of the helix I do not interact with the hydrophobic amino acids of the C-terminal part of helix IV. After the simulation, the interface between the N-terminal half of helix I and the C-terminal half of helix IV is stabilized by different, but mostly non-polar interactions involving amino acids Glu5, Met8 and Ile12 from helix I and Ala79, Thr82 and His86 from helix IV (Fig. 6). After the simulation, the resulting structure has an additional hydrogen bond between Glu5 and Ser83, which provides an additional stabilization of the contact interface. Moreover, molecular dynamics calculations show that after the monomer separation the lost contacts at the dimer interface are reformed inside each monomer with equivalent new interactions. Indeed, before simulation, amino acids Glu5, Met8 and Ile12, which belong to helix I in chain A, interact with Val78, Thr82 and His86 from helix IV' (chain B), and Glu5 (helix I, chain A) forms a hydrogen bond with Ser85 (helix IV', chain B) (Fig. 7). After the simulation, helix I (chain A) approaches the position of helix I' (chain B), and the same amino acids Glu5, Met8 and Ile12 of helix I (chain A) interact with Ala79, Thr82 and His86 of helix IV (chain A), while Glu5 (helix I, chain A) forms a hydrogen bond with Ser83 (helix IV, chain A) (Figs. 5 and 6). As a result, all interactions that stabilized the

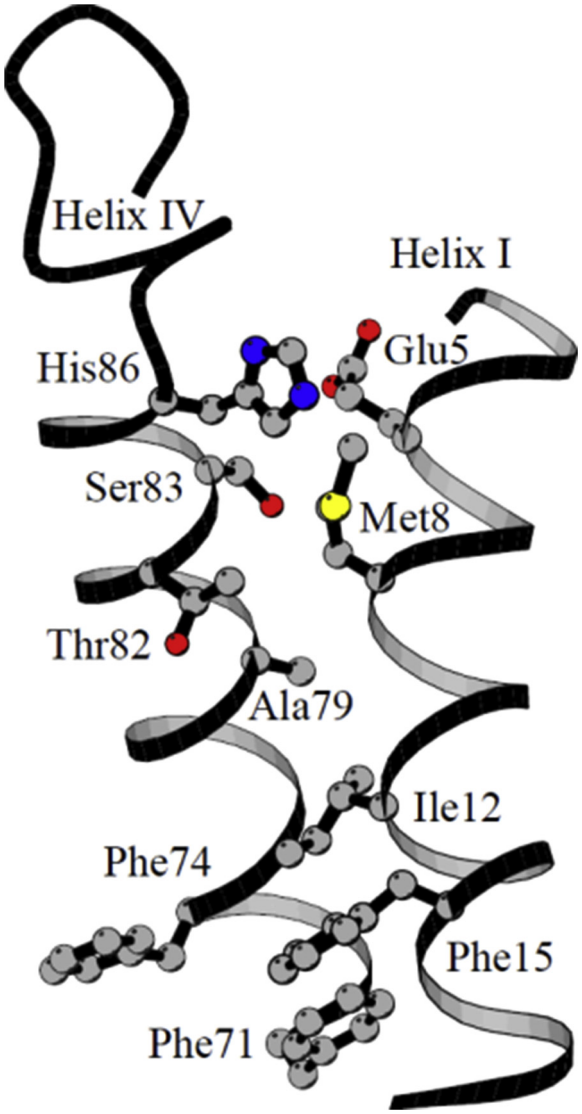

Fig. 6. A network of non-polar interactions between Helices I and IV stabilize the monomer structure of the S100P protein after the 80 ns molecular dynamics simulation.

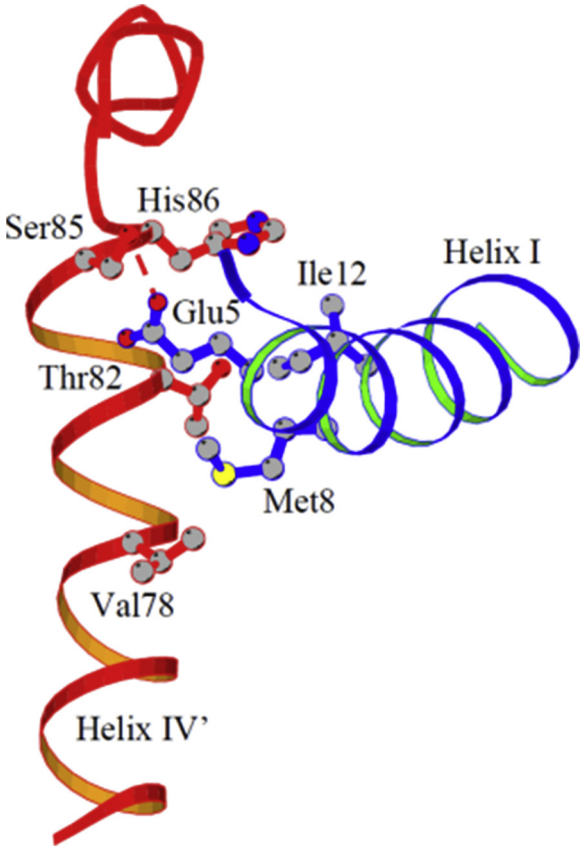

Fig. 7. Cluster of interacting non-polar residues between Helices I and IV' stabilize the apo-S100P homodimer structure before the 80 ns molecular dynamics simulation.

interdomain interface in the S100P homodimer are reformed in each separated monomer after the structural rearrangement. Finally, the molecular dynamics simulation showed that the contact area between helices I and IV' of the S100P homo-dimer is 345 Å^2 and it coincides with the area between helices I and IV of the resulting S100P monomer after the simulation, 387 Å^2. It shows that separated S100P monomer in the solution tries to rearrange its structure to mimic conformational settings of the four-helix bundle characteristic for its homodimer.

To analyze how far the rearranged simulated S100P monomer deviates from the starting structure, we used the GROMACS 'g_rmsf' tool. This tool computes the Root Mean Square Fluctuation (RMSF), i.e. standard deviation of atomic positions of the multitude of the molecular dynamics results with respect to the starting conformation Fig. 8 [25]. The RMSF results show that the N-terminal part of helix I and the C-terminal part of helix IV have maximal flexibility, which is consistent with the data presented above.

Earlier we showed that all EF-hand calcium-binding domains contain a highly-conserved three-residue aromatic structural motif, which consists of one amino acid from the C-terminus of helix I and two amino acids from the N-terminus of helix IV [38]. These conserved amino acids in S100P are Phe15, Phe71 and Phe74, and the results of the present study show that they display the lowest flexibility (Figs. 6 and 8), which is in line with our earlier suggestions [38].

Thus, the molecular dynamics simulations show that the separated S100P monomer can have a compact globular structure. The main change of the 3D structure of the separated S100P monomer is a rotation of its helix I with respect to helix IV. The axis of such rotation can go through the conserved aromatic cluster (Phe15, Phe71 and Phe74 in S100P), which is a universal feature of all EF-hand domains [38]. In the resulting monomeric structure after the 80-ns simulation, an interface between helices I and IV contains the same set of interacting hydrophobic amino acids as the interface between helices I and IV' (from two different monomers) in the original homodimer structure before the simulation. The results of the simulation for the chain B of the homodimer are the same as for the chain A (data not shown). Similar results were obtained also for S100B and S100A11 proteins.

For molecular dynamics calculations, we have chosen the structure of bovine S100B in the calcium-free state (PDB Code: 1CFP; model 1; chain A [29]. Conformational changes in the separated S100B monomer during the 80-ns molecular dynamics simulation involve the entire structure, but similarly to S100P, the most pronounced changes occur in the relative orientation of helices I and IV. Similarly to S100P, in S100B, rotation of helix I around helix IV results in changes in the aromatic cluster, Phe14 (helix I), Phe70 (helix IV) and Phe73 (helix IV), which was shown to be conserved in all EF-hand calcium-binding domains [38]. Rotation of helices I and IV causes an appearance of a new non-polar interface, including the aliphatic portion of the side-chain of Glu2, and the side-chains of Leu3, Val7, Ile11 (all from helix I) and the side-chains of Val77, Thr81 and Phe87 (all from helix IV). In the S100B homodimer, the same set of hydrophobic amino acids, Leu3, Val7 and Ile11, forms the dimer interface and interacts with the equivalent amino acids, Val77, Thr81 and Phe 87 from helix IV' (chain B).

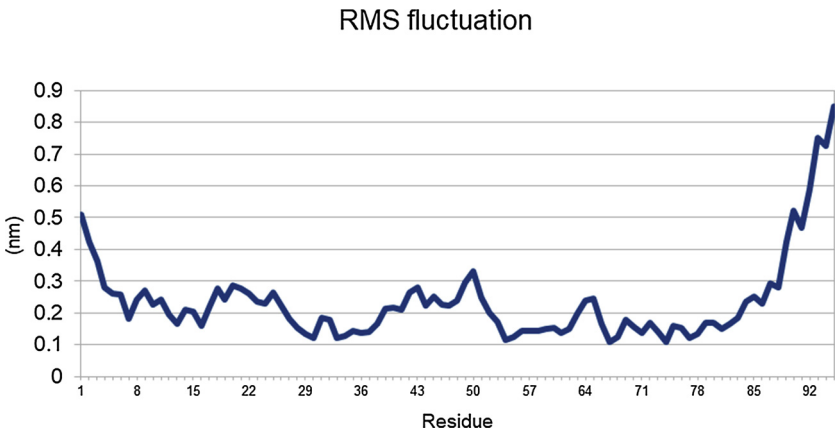

Fig. 8. Resulting deviation of atomic positions of all obtained molecular dynamics results for all amino acids of S100P.

Moreover, an aromatic cluster between helices I and IV' of the homodimer (Phe14, Phe87 and Phe88) is formed in the S100B monomer (Phe14, Phe70 and Phe73). Thus, an analysis of the changes, which occur during the 80-ns molecular dynamics simulation shows formation of a hydrophobic core of the S100B monomeric protein. The helices I and IV are rearranged to fully mimic all lost non-polar interactions in the dimer interface. Moreover, similar to S100P, a new contact is formed between Glu2 and Phe87.

The contact area between helices I and IV' of the S100B homodimer and the area between helices I and IV of the S100B monomer after the 80-ns simulation do also coincide (434 $Å^2$ in the dimer and 421 $Å^2$ in the monomer, respectively). Similar to S100P, the RMSF calculations show that after the 80-ns molecular dynamics simulation, the axis of the conserved hydrophobic cluster Phe14, Phe70 and Phe73 remains immobile, while the rest of helices I and IV change their relative conformation. These results are also consistent with the changes in S100P.

We also made similar molecular dynamics calculations for the third known apo-S100 dimer, S100A11 (PDB code: 1NSH, conformer 1; [30]. Initial conditions and settings for the S100A11 set of calculations were also similar to those described above for S100P and S100B. Molecular dynamics calculations during 80 ns time interval showed conformational rearrangement of helices I and IV identical to those seen in S100P and S100B. Particularly, in S100A11 we observed convergence of the two helices following the rotation around the axis going through the conserved aromatic cluster Phe17, Phe73 and Phe76, with the resulting formation of a new hydrophobic interface between helices I and IV. The amino acid content of the hydrophobic interface between helices I and IV is the same as the one between helices I and IV' in the apo-S100A11 dimer. However, in S100A11, the size of the interface between helices I and IV significantly increases as a result of 80-ns simulation: 469 $Å^2$ in the monomer versus 369 $Å^2$ in the dimer, which suggests a tighter structure of S100A11 in comparison to those of S100P and S100B.

Molecular dynamics results shown above are in line with the structural data obtained earlier in the work on oxidative labeling and mass spectrometry of S100A11 protein at pH 2 [39]. In this work, the authors showed that at pH 2 the monomer compensates the loss of intermolecular contacts between helices I and IV by formation of new intramolecular contacts. Particularly, it was demonstrated that the hydrophobic amino acids Leu13, Ile14 and Val16 from helix I and amino acids Leu77 and Ile80 from helix IV are packed against each other in the structure of acid-denatured monomeric S100A11 [39].

Conflict of interest statement

We, Sergei E. Permyakov, Alexander I. Denesyuk, Konstantin A. Denessiouk, Maria E. Permyakova, Alixey S. Kazakov, Ramis G. Ismailov, Victoria A. Rastrygina, Andrei S. Sokolov, Eugene A. Permyakov, authors of the manuscript entitled "Monomeric state of S100 P protein: experimental and molecular dynamics study.", wish to confirm that there are no known conflicts of interest associated with this publication and there has been no significant financial support for this work that could have influenced its outcome.

Acknowledgements

This work was supported by a grant NK 15-04-05966 from the Russian Fund of Basic Research. Computational infrastructure was provided by Biocenter Finland Bioinformatics) and by grants from the Sigrid Juselius Foundation.

Appendix A. Supplementary data

Supplementary material related to this article can be found, in the online version, at doi:https://doi.org/10.1016/j.ceca.2019.04.008.

References

[1] R. Donato, S100: a multigenic family of calcium-modulated proteins of the EF-hand type with intracellular and extracellular functional roles, Int. J. Biochem. Cell Biol. 33 (2001) 637–668.
[2] R. Donato, C.L. Geczy, D.J. Weber, S100 proteins, in: R. Kretsinger, V.N. Uversky, E.A. Permyakov (Eds.), Encyclopedia of Metalloproteins, Springer Science +Business Media, New York, 2013, pp. 1863–1874.
[3] E.A. Permyakov, R.H. Kretsinger, Calcium Binding Proteins, John Wiley & Sons, Inc, Hoboken, New Jersey, 2011.
[4] D. Kligman, D.C. Hilt, The S100 protein family, Trends Biochem. Sci 13 (1988) 437–443.
[5] T. Becker, V. Gerke, E. Kube, K. Weber, S100P, a novel Ca(2+)-binding protein from human placenta. cDNA cloning, recombinant protein expression and Ca2+ binding properties, Eur. J. Biochem. 207 (1992) 541–547.
[6] Y. Emoto, R. Kobayashi, H. Akatsuka, H. Hidaka, Purification and characterization of a new member of the S-100 protein family from human placenta, Biochem. Biophys. Res. Commun. 182 (1992) 1246–1253.
[7] H. Jiang, H. Hu, X. Tong, Q. Jiang, H. Zhu, S. Zhang, Calcium-binding protein S100P and cancer: mechanisms and clinical relevance, J. Cancer Res. Clin. Oncol. 138 (2012) 1–9.
[8] V. Tothova, A. Gibadulinova, S100P, a peculiar member of S100 family of calcium-binding proteins implicated in cancer, Acta Virol. 57 (2013) 238–246.
[9] R.L. Eckert, A.M. Broome, M. Ruse, N. Robinson, D. Ryan, K. Lee, S100 proteins in the epidermis, J. Invest. Dermatol. 123 (2004) 23–33.
[10] P. Cancemi, G. Di Cara, N.N. Albanese, F. Costantini, M.R. Marabeti, R. Musso, C. Lupo, E. Roz, I. Pucci-Minafra, Large-scale proteomic identification of S100 proteins in breast cancer tissues, BMC Cancer 10 (2010) 476.
[11] Y. Tutar, Dimerization and ion binding properties of S100P protein, Protein Pept. Lett. 13 (2006) 301–306.
[12] H. Zhang, G. Wang, Y. Ding, Z. Wang, R. Barraclough, P.S. Rudland, D.G. Fernig, Z. Rao, The crystal structure at 2A resolution of the Ca2+ -binding protein S100P, J. Mol. Biol. 325 (2003) 785–794.
[13] M. Koltzscher, V. Gerke, Identification of hydrophobic amino acid residues involved in the formation of S100P homodimers in vivo, Biochemistry 39 (2000) 9533–9539.
[14] M.E. Permyakova, A.S. Kazakov, A.I. Denesyuk, K.A. Denesyuk, E.A. Permyakov, Analyzing the structural and functional roles of residues from the 'black' and 'gray' clusters of human S100P protein, Cell Calcium (2019).
[15] A.S. Kazakov, A.S. Sokolov, V.A. Rastrygina, V.V. Solovyev, R.G. Ismailov, R.V. Mikhailov, A.B. Ulitin, A.R. Yakovenko, T.A. Mirzabekov, E.A. Permyakov,

S.E. Permyakov, High-affinity interaction between interleukin-11 and S100P protein, Biochem. Biophys. Res. Commun. 468 (2015) 733–738.
[16] C.N. Pace, F. Vajdos, L. Fee, G. Grimsley, T. Gray, How to measure and predict the molar absorption coefficient of a protein, Protein Sci. 4 (1995) 2411–2423.
[17] H.E. Blum, P. Lehky, L. Kohler, E.A. Stein, E.H. Fischer, Comparative properties of vertebrate parvalbumins, J. Biol. Chem. 252 (1977) 2834–2838.
[18] E.A. Permyakov, E.A. Burstein, Some aspects of studies of thermal transitions in proteins by means of their intrinsic fluorescence, Biophys. Chem. 19 (1984) 265–271.
[19] E.A. Permyakov, Luminescent Spectroscopy of Proteins, CRC Press, Boca Raton, Ann Arbor, London, Tokyo, 1993.
[20] P.L. Privalov, S.A. Potekhin, Scanning microcalorimetry in studying temperature-induced changes in proteins, Methods Enzymol. 131 (1986) 4–51.
[21] M. Hackel, H.J. Hinz, G.R. Hedwig, Partial molar volumes of proteins: amino acid side-chain contributions derived from the partial molar volumes of some tripeptides over the temperature range 10-90 degrees C, Biophys. Chem. 82 (1999) 35–50.
[22] G.I. Makhatadze, P.L. Privalov, Heat capacity of proteins. I. Partial molar heat capacity of individual amino acid residues in aqueous solution: hydration effect, J. Mol. Biol. 213 (1990) 375–384.
[23] S.E. Permyakov, A.G. Bakunts, M.E. Permyakova, A.I. Denesyuk, V.N. Uversky, E.A. Permyakov, Metal-controlled interdomain cooperativity in parvalbumins, Cell Calcium 46 (2009) 163–175.
[24] Y.C. Lee, D.E. Volk, V. Thiviyanathan, Q. Kleerekoper, A.V. Gribenko, S. Zhang, D.G. Gorenstein, G.I. Makhatadze, B.A. Luxon, NMR structure of the Apo-S100P protein, J. Biomol. NMR 29 (2004) 399–402.
[25] B. Hess, C. Kutzner, D. van der Spoel, E. Lindahl, GROMACS 4: algorithms for highly efficient, load-balanced, and scalable molecular simulation, J. Chem. Theory Comput. 4 (2008) 435–447.
[26] H.J. Berendsen, J.R. Grigera, The missing term in effective pair potentials, J. Phys. Chem. 91 (1997) 6269–6271.
[27] H.J.C. Berendsen, J.P.M. Postma, A. DiNola, J.R. Haak, Molecular dynamics with coupling to an external bath, J. Chem. Phys. 81 (1984) 3684–3690.
[28] U. Essmann, L. Perera, M.L. Berkowitz, T. Darden, H. Lee, L.G. Pederson, A smooth particle meshes Ewald potential, J. Chem. Phys. 103 (1995) 8577–8592.
[29] P.M. Kilby, L.J. Van Eldik, G.C. Roberts, The solution structure of the bovine S100B protein dimer in the calcium-free state, Structure 4 (1996) 1041–1052.
[30] A.C. Dempsey, M.P. Walsh, G.S. Shaw, Unmasking the annexin I interaction from the structure of Apo-S100A11, Structure 11 (2003) 887–897.
[31] V. Sobolev, A. Sorokine, J. Prilusky, E.E. Abola, M. Edelman, Automated analysis of interatomic contacts in proteins, Bioinformatics 15 (1999) 327–332.
[32] M. Ernst, T.L. Putoczki, Molecular pathways: IL11 as a tumor-promoting cytokine-translational implications for cancers, Clin. Cancer Res. 20 (2014) 5579–5588.
[33] T.L. Putoczki, M. Ernst, IL-11 signaling as a therapeutic target for cancer, Immunotherapy 7 (2015) 441–453.
[34] E.A. Permyakov, V.N. Uversky, S.E. Permyakov, Interleukin-11: a multifunctional cytokine with intrinsically disordered regions, Cell Biochem. Biophys. 74 (2016) 285–296.
[35] T. Arumugam, C.D. Logsdon, S100P: a novel therapeutic target for cancer, Amino Acids 41 (2011) 893–899.
[36] A.S. Kazakov, M.P. Shevelyova, R.G. Ismailov, M.E. Permyakova, E.A. Litus, E.A. Permyakov, S.E. Permyakov, Calcium-dependent interaction of monomeric S100P protein with serum albumin, Int. J. Biol. Macromol. 108 (2018) 143–148.
[37] H.M. Berman, J. Westbrook, Z. Feng, G. Gilliland, T.N. Bhat, H. Weissig, I.N. Shindyalov, P.E. Bourne, The protein data bank, Nucleic Acids Res. 28 (2000) 235–242.
[38] K. Denessiouk, S. Permyakov, A. Denesyuk, E. Permyakov, M.S. Johnson, Two structural motifs within canonical EF-hand calcium-binding domains identify five different classes of calcium buffers and sensors, PLoS One 9 (2014) e109287.
[39] B.B. Stocks, A. Rezvanpour, G.S. Shaw, L. Konermann, Temporal development of protein structure during S100A11 folding and dimerization probed by oxidative labeling and mass spectrometry, J. Mol. Biol. 409 (2011) 669–679.
[40] S. Tarabykina, D.J. Scott, P. Herzyk, T.J. Hill, J.R. Tame, M. Kriajevska, D. Lafitte, P.J. Derrick, G.G. Dodson, N.J. Maitland, E.M. Lukanidin, I.B. Bronstein, The dimerization interface of the metastasis-associated protein S100A4 (Mts1): in vivo and in vitro studies, J. Biol. Chem. 276 (2001) 24212–24222.
[41] G. Wang, S. Zhang, D.G. Fernig, M. Martin-Fernandez, P.S. Rudland, R. Barraclough, Mutually antagonistic actions of S100A4 and S100A1 on normal and metastatic phenotypes, Oncogene 24 (2005) 1445–1454.
[42] X.J. Gong, X.Y. Song, H. Wei, J. Wang, M. Niu, Serum S100A4 levels as a novel biomarker for detection of acute myocardial infarction, Eur. Rev. Med. Pharmacol. Sci. 19 (2015) 2221–2225.
[43] W.W. Streicher, M.M. Lopez, G.I. Makhatadze, Modulation of quaternary structure of S100 proteins by calcium ions, Biophys. Chem. 151 (2010) 181–186.
[44] J. Zhang, K. Zhang, X. Jiang, S100A6 as a potential serum prognostic biomarker and therapeutic target in gastric cancer, Dig. Dis. Sci. 59 (2014) 2136–2144.
[45] X.Y. Cai, L. Lu, Y.N. Wang, C. Jin, R.Y. Zhang, Q. Zhang, Q.J. Chen, W.F. Shen, Association of increased S100B, S100A6 and S100P in serum levels with acute coronary syndrome and also with the severity of myocardial infarction in cardiac tissue of rat models with ischemia-reperfusion injury, Atherosclerosis 217 (2011) 536–542.
[46] B. Meijer, R.B. Gearry, A.S. Day, The role of S100A12 as a systemic marker of inflammation, Int J Inflam (2012) 907078.